Eco. Env. & Cons. 28 (January Suppl. Issue) : 2022; pp. (S54-S61)

ISSN 0971–765X

http://doi.org/10.53550/EEC.2022.v28i01s.007

An experimental investigation to the use of Calcium Chloride in the water body construction of a salinity gradient solar pond

Wael Chasib Thwayin, Mohammed A. Altahan and Asaad H. Sayer

Department of Chemistry, College of Science, University of Thi-Qar, Iraq

(Received 30 July, 2021; Accepted 6 September, 2021)

ABSTRACT

In this paper, calcium chloride was used to construct the water body of a small salinity gradient solar pond (SGSP). The study was carried out from the 1st of November to 10th of June 2021 in Nasiriya City, South of Iraq. The pond had a cylindrical shape with a surface area of 0.19625 m^2, and a depth of 1 m. The results showed that calcium chloride can be used effectively in the construction of the SGSPs. The highest temperature was 59 ºC in June.

Key words : *Calcium Chloride solar pond salinity gradient*

Introduction

A salinity-gradient solar pond (SGSP) (Fig. 1) is a large body of water with a depth between 2 and 5 m and a salinity gradient. Solar radiation reaches the bottom of the pond is trapped in the lower region and stored, this because convection currents in the middle layer of the pond are suppressed. The pond basically consists of three layers, the upper convective zone (UCZ), it has low salinity brine. Below the UCZ, the non-convective zone (NCZ), it is constructed with a salinity gradient from top to bottom. It works as a transparent thermal insulator since natural convection currents are suppressed. The third layer or zone is the lower convective zone (LCZ), it is also known as the storage zone (Hull *et al.*, 1988; Leblanc *et al.*, 2011; Akbarzadeh *et al.*, 2008; Hassairi *et al.*, 2001).

SGSPs can supply reliable thermal energy at temperatures between 50 and 90 ºC and have a low capital cost (Andrews and Akbarzadeh, 2005).

The most salts used in SGSPs are Sodium Chloride (NaCl), Magnesium Chloride ($MgCl_2$) and fertilizer salts. At the beginning,, natural brine was used, in this case the maximum temperature obtained was less than in the case of sodium chloride pond (Hassairi *et al.*, 2001). magnesium chloride ($MgCl_2$) is used in SGSPs, it is considered as the second largest salt constituent of sea and ocean water, although it is the largest proportion of salt in the Dead Sea. This

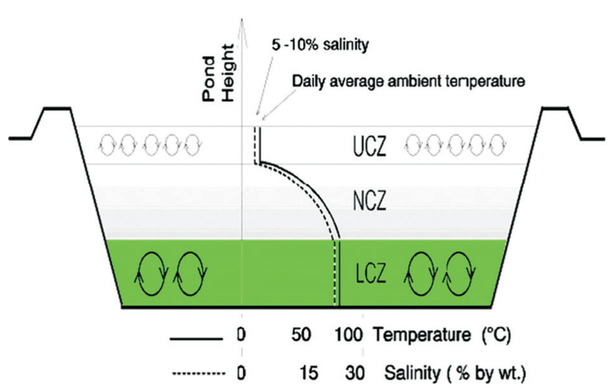

Fig. 1. Schematic of a salinity gradient and temperature profiles (Leblanc *et al.*, 2011).

salt is exceptionally stable during operation; it also exhibits great solubility in producing brine with high density, as it can dissolve between 35 and 40% depending on the solution temperature (Tabor, 1979; Ochs *et al.*, 1981).

The possibility of using fertilizers such as ammonium salts in solar ponds was investigated. It was visualized that a solar pond system integrated with the farm, in which the heat extracted from the SGSP may be used for the crop drying, water and space heating, or other low-temperature applications. Some of the fertilizer salts are nitrogenous fertilizers such as ammonium nitrate, ammonium sulfate, ammonium chloride, ammonium phosphate, ammonium superphosphate, ammonium orthophosphate, and ammonium polyphosphate. other studies were performed on some other salts (Hull, 1986; Murthy and Pandey, 2002; Kurt *et al.*, 2006).

In the present study, the thermal performance of a small SGSP was experimentally investigated when $CaCl_2.2H_2O$ is used in the construction of the salinity gradient.

Experimental unit

The study was carried out from 01/11/2020-10/06/2021 (222 days). A small SGSP with a surface area of 0.19625 m^2, and a depth of 1 m was constructed in Nasiriyah City, south of Iraq (Latitude: 31.0510°, Longitude: 46.2569°).

The experimental unit was a cylindrical tank made of plastic with a thickness of 1 cm. The side walls and base of the tank were surrounded by a wooden frame of with a thickness of 2 and 3 cm for the side walls and base respectively. In between the thermal insulation was constructed with two layers, a layer of polyurethane (6 cm thick) and a layer polystyrene (10 cm thick) which acted as an insulator. The small pond was mounted on a plastic base with a height of 10 cm. The inner sides of the pond

Fig. 2. Pictures of the experimental SGSP.

were painted black, providing an anti-corrosion barrier, and increasing the solar radiation absorptivity. Figures 2 and 3 show pictures of the experimental SGSP, and a schematic of the experimental unit.

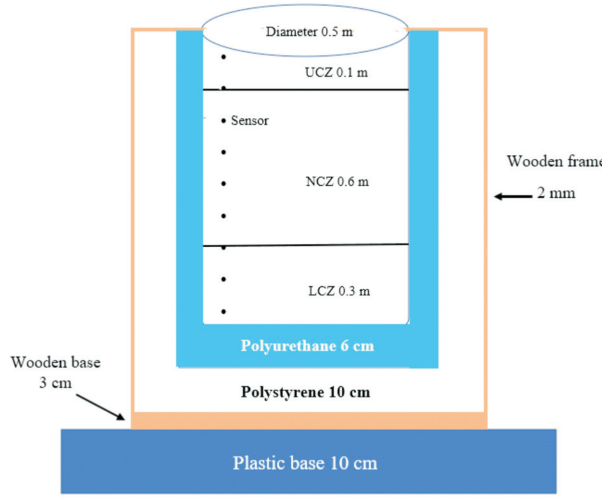

Fig. 3. Schematic diagram showing the cross-section for SGSP, with the distribution of the thermocouples which monitor the Spatio-temporal evolution of the temperature field within the pond.

Water body construction

The method used in the water body construction was similar to those used by Suárez *et al.*, 2014; Aizaz and Yousaf, 2013; and Sayer *et al.*, 2017. A solution with high salt ($CaCl_2.2H_2O$) concentration (0.22 kg/l) was prepared in a mixing tank. Then the prepared solution was transferred to the experimental pond by a small pump. The layer had a depth of 0.3 m.

The NCZ was established by adding many layers of salty water whose salt concentration (and hence density) decreased from the top of the LCZ toward the UCZ. For this purpose, four 15 cm layers of varying salt concentration (0.17, 0.12, 0.07, and 0.02 kg/l) were added consecutively to the top of the LCZ. This formed the NCZ with a total depth of 0.6 m. At the end of the pipe which transferred the salty water from the mixing tank to the pond, a shower with small holes (of 0.4 mm in diameter) was used to add the water to the pond with minimal momentum. the flow rate was 0.25 l/min to minimised any disturbance of the layers.

The final layer, the UCZ, it had a thickness of 0.1 m and was created with fresh water. The water level and Fig. 4 shows schematically the system which was used in the water body formation. Water was poured using the shower onto a layer of polystyrene with a thickness of 10 cm, as shown in Fig. 4.

Data collection

Measurements of temperature

The data acquisition system consists of a set of thermocouples (K type; coated for the corrosion protection) installed at various elevations in the pond. A data reader (Autonics TCN4H-24R) is used to measure the temperatures. The experimental temperature distributions were measured using 9 calibrated K-type thermocouples.

The thermocouples were fixed along the vertical centreline of the inner zones of the pond to measure the temperature profiles of the three zones (UCZ, NCZ, and LCZ). Thermocouples were located, measuring from the bottom of the pond to the edge of the LCZ, at heights of 0.05, 0.15, and 0.3 m. Five sensors were placed in the NCZ (0.38, 0.53, 0.68, 0.83, and 0.9 m), and for the UCZ, a single thermocouple was fixed to measure the temperature there. All thermocouples were connected to a control board with a digital reader by 2 m extension wires.

Concentration measurements

In this study, the sample weighing method was used. 10 ml of the drawn sample is heated to evaporate water, after that, the sample was completely dried, and weighed. This method is simple, effective, and inexpensive.

Samples were taken from the three zones of the pond. The concentrations of these samples were measured directly after they were taken from the pond. For the NCZ, a sample from each layer was taken (0.38, 0.53, 0.68, and 0.83 m), and for the LCZ, samples were taken from depths of 0.05, 0.15, and 0.25 m, and one sample was taken from the UCZ layer (0.98 m). Samples were taken using the tool shown in Fig. 5.

Fig. 5. The instrument used for sampling. Its syringe (20 ml) is installed and connected to a covered iron screw (110 cm).

Turbidity and pH measurements

In this study, the turbidity of water samples was measured by using the device of Multi-Direct. Firstly, the device was adjusted with distilled water, then samples were tested.

For the PH, samples were drawn from different depths and the pH was measured for the mixture. After each measurement, the pH electrode was cleaned with fresh water to remove the salt. A HANNA pH 211 device was used for measuring pH.

Results and Discussion

Concentration measurements

Concentration measurements are illustrated in Fig. 6 for eight different days.

Fig. 6 shows that after 10 days, there was a clear salinity gradient. The salinity was high in the LCZ

Fig. 4. Experimental system of building water body. (a) The shower (b) Mixing tank and pump.

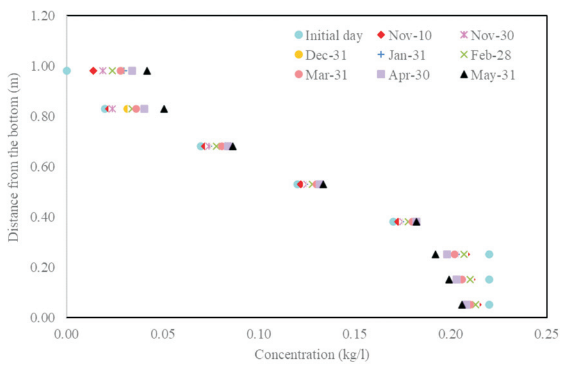

Fig. 6. Salinity gradient of SGSPs for eight different days.

(0.211 kg/l) and then there was a concentration gradient along the NCZ and at the top of the pond, a little salinity in the UCZ (0.014 kg/l) was apparent. After 30 days, a large decrease in the concentration of LCZ has occurred. Moreover, on December 31, the figure shows that there was a decrease and increase in the salinity of the LCZ and UCZ respectively. The prevalence rate decreases on January 31 and February 28 compared to what it was on December 31 and then increases again starting from March 31 to reach its maximum on May 31. Salt was injected on the days indicated in Fig. 6 to compensate the decrease in the concentration of LCZ according to the method proposed by Date and Akbarzadeh (2013). Fig. 7 shows the concentration measurements for UCZ and the top layer of the NCZ, which are located directly below it.

Fig. 7 shows that there is an increase in the concentration of the top layer of the NCZ over time. The behaviour of UCZ was identical, except for the period of 120-151 when the prevalence rate was lower. As of day 10, the surface of the pond was washed with fresh water roughly every five days to control

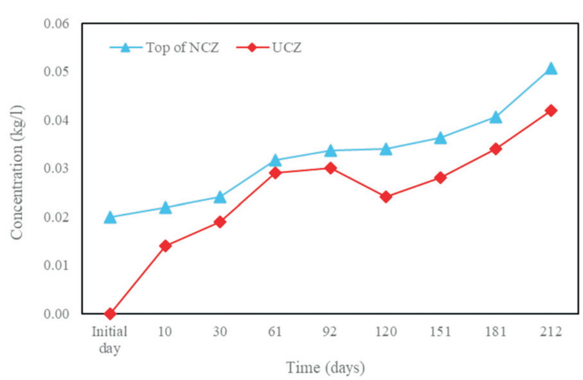

Fig. 7. Concentrations of the UCZ and the top layer of the NCZ.

the salinity level. The experiment clearly showed the necessity of regular surface washing to prevent instability due to salinity disturbance. During days 151–212, disturbances in the concentration profiles at different pond layers were observed. It appears that the rise in temperature during hot seasons not only affected the evaporation rate but also increased the salt diffusion rate, which in return required a more regular surface washing. Hull et al. (1988) reported that, depending on the experiences collected from some SGSPs, it was estimated that the upward salt diffusion can be about 40 kg/m^2 year in the hot and sunny climate. The results concluded that the concentration of LCZ generally has decreased, and there is a change in the concentration of LCZ with depth. Fig. 8 illustrates the change in concentration of the LCZ with its depth.

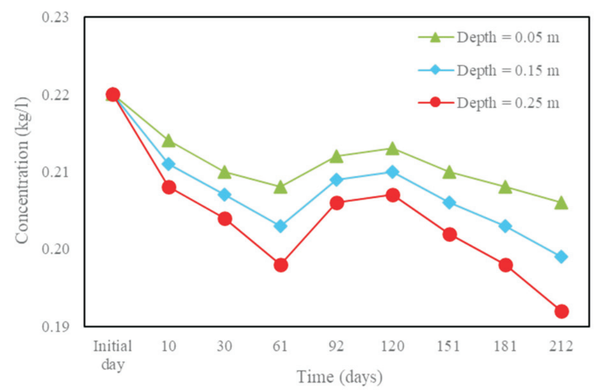

Fig. 8. Change in concentrations of the LCZ with depth. The depths considered are 0.05, 0.15, and 0.25 m.

It is evident from Fig. 8 that the change in the concentration of the LCZ decreases with its depth. The depth of the LCZ in the pond was 0.3 m and this depth is small. In other words, the rate of diffusion from the surface of the LCZ is greater than from its bottom, which leads to erosion of the NCZ.

Turbidity and brine transparency

Brine transparency is an important part of the maintenance of a salinity gradient solar pond as it affects the amount of solar radiation reaching the storage zone and hence has an influence on the thermal performance. After five days of the beginning of the operation, the ponds became clear, and this period was relatively long. It may be due to the small surface area of the pond compared to their depth. After this period, it became possible to see the bottom of the pond, as shown in Fig. 9.

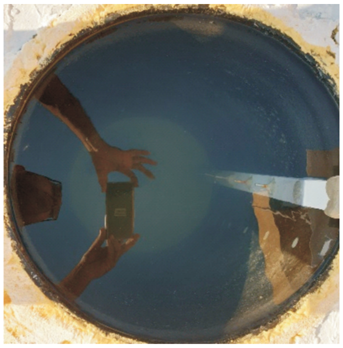

Fig. 9. Transparency of brine for experimental ponds after five days of operation.

Throughout the study period, two factors that affected the clarity of the ponds were observed: The first factor is rain, which results in a significant decrease in the clarity due to the mixing of water on the surface of the ponds. The second factor is the dust storms, which had the greatest effect on the transparency of the brine. Fig. 10 shows the turbidity profile of the pond before and after treatment for the specified period from November 5 to June 1.

Fig. 10 shows that the turbidity in the fifth day of the start of the operation was 0.7 NTU, and then began to rise gradually. The reason for this increase is the rain on the days of 12, 20, 21, and 29 November and 1, 2, 5, and 6 December. On day 37, December 7, the first treatment was carried out using alum, which was dissolved ~2.5 g in 250 ml of distilled water and the solution was poured quietly and gently over the surface of the pond. In other words, the concentration of alum in the pond became 0.0125 g/l. A clear decrease in the turbidity of the brine after 5 days of treatment was noticed, and the turbidity of the pond was acceptable during the period of 42-107 days, where the bottom of the pond can be seen

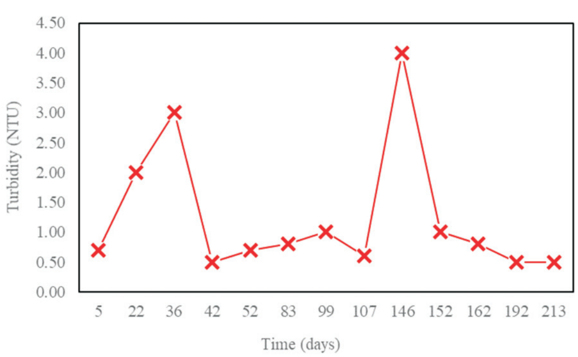

Fig. 10. The turbidity profile of the pond before and after treatment.

clearly. In the period from February 15 to March 26, there were thick waves of dust that caused the turbidity to rise significantly.

The second treatment was carried out on the pond on March 27 using where sodium dichloroisocyanurate was used as a source of chlorine. Initially, alum was used at the same concentration as before (0.0125 g/l) for the purpose of precipitating solids, then chlorination of the brine solution at a concentration of 5.8 mg/l to treat algae. After the second treatment, a clear decrease in the turbidity was noticed of the water body (the period of 152-213 days in Fig. 10). In both treatments, the brine for the pond was acidified by pouring 400 ml of HCl (0.05N). The pH profile is shown in Fig. 11. Sodium dichloroisocyanurate ($C_3Cl_2N_3NaO_3$) is a good source of chlorine, as it has a low pH (6.4-6.6) and does not cause corrosion, and in order to work effectively, the water must be clean. Therefore, alum was initially used to precipitate solids. In general, it is a better alternative than sodium hypochlorite, which has a high pH (7.2-10.6) in addition to being corrosive.

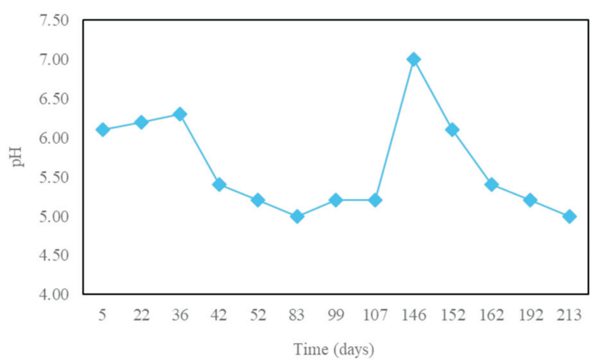

Fig. 11. The pH profile of experimental pond.

Fig. 11 shows that pH measurements are necessary, as high values may indicate that the pond environment has become perfect for the growth of bacteria and algae. In many cases, the pH values are in positive agreement with the turbidity values.

Temperature profile

LCZ temperature development

The temperature evolution in the storage zone is shown in Fig. 12.

Fig. 12 shows the ideal positive correlation between LCZ temperature, solar radiation, and ambient temperature. In November (the first month of the operating period), the monthly mean of the LCZ

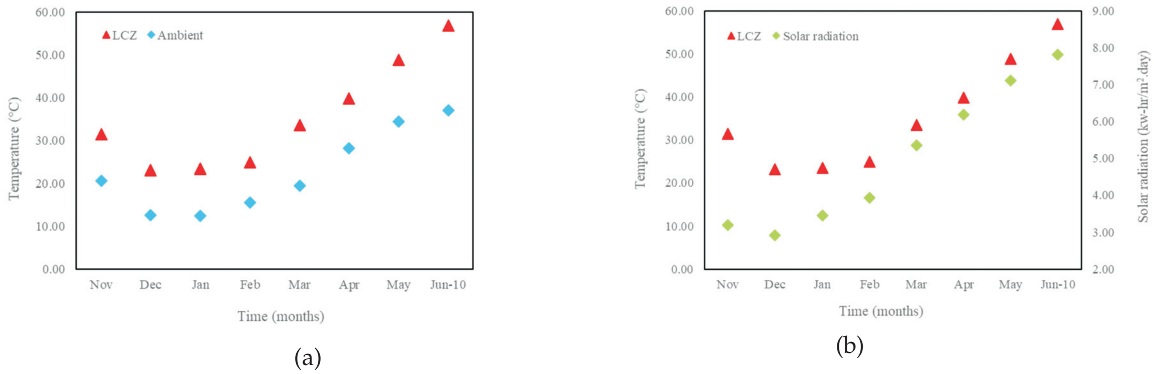

Fig. 12. Monthly average of LCZ temperature and (a) the ambient temperature (b) solar radiation, at midday from November 1 to June 10.

temperature was 31.53 °C, while the water temperature used to construct the ponds was 26°C. In the sense that there is a noticeable increase in the temperature of the storage zone, even though the weather is moderate. The weather in general shifts towards the cold season, and the features of this shift are evident in the LCZ temperature, especially in December, when the ponds record the lowest temperature during the study period, with a significant difference of 8.35 °C from November. The small surface area of the ponds (0.5m) greatly affected the temperature of the LCZ in the cold season, while the features of recovery appeared clearly in March, and the increase in the temperature of the LCZ continued with time to reach its maximum rate in June (56.9 °C).

UCZ temperature development

The temporal temperature development in the UCZ, the ambient temperature, and solar radiation are shown in Fig. 13.

Fig. 13 illustrates that the temperature of the UCZ was lower than the ambient temperature and its variation was like that of the ambient temperature. This behaviour is because the UCZ receives heat from the LCZ by conduction and some of the incident solar radiation accumulates in this layer. However, the layer also loses heat to the atmosphere through radiation, convection, and evaporation. The temperature in the UCZ tended to be lower than the ambient air in the daytime

Temperature variation with depth

The change in temperature profile within the pond is shown in Fig. 14.

Many interesting features can be identified in Figure 14. Firstly, the LCZ temperature continued to increase, reaching its maximum in June. Interestingly, there was also a growth in the UCZ temperature and the difference between the two temperatures on June 10 was 20.5 °C. Secondly, it is also interesting to note that, there was a clear and uniform

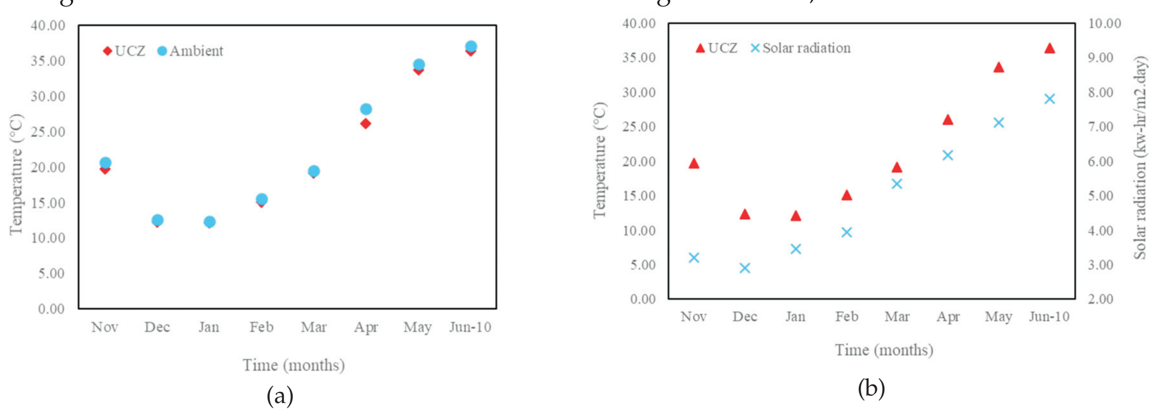

Fig. 13. Average monthly temperature for UCZ and (a) the ambient temperature (b) solar radiation, at midday between November 1 and June 10.

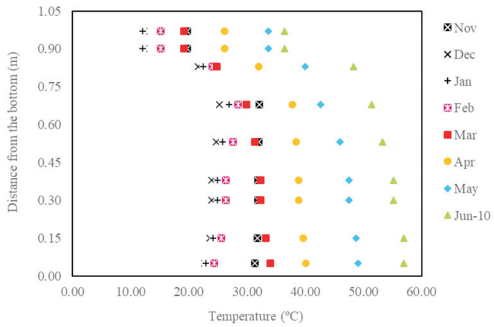

Fig. 14. Temperature distribution in the pond.

temperature gradient through the NCZ. But it was generally slight among some layers. Especially in the lowest layers of the pond, the reason may be that not a large amount of solar radiation reaches due to the small surface area of the pond, which makes the effect of shadowing the walls is great, especially in the cold season. Finally, the results in Fig. 14 can be divided into two periods. The first is from November to February, when the temperature of NCZ is higher creases from the bottom of the pond to a depth of 0.68 m, and the second is from March to June, where the temperature increases linearly from the top to the bottom of the pond, as shown in Fig. 15.

The change in the behaviour of the temperature distribution inside the pond, shown in Fig. 15, occurs as a result of the improvement in the angle of incidence of solar radiation on the pond. The incidence angles of solar radiation on the pond are illustrated in Fig. 16.

It is illustrated in Fig. 16 that if the surface area was larger, the amount of heat accumulated in the storage zone (LCZ) would be greater.

Conclusion

Calcium chloride brine is the best at absorbing solar radiation and is most affected by the ambient temperature. It is characterized by rapid heating as well as rapid cooling. The cooling rate between night and day was 3.55 °C in the cold season and 2 °C in the hot season.

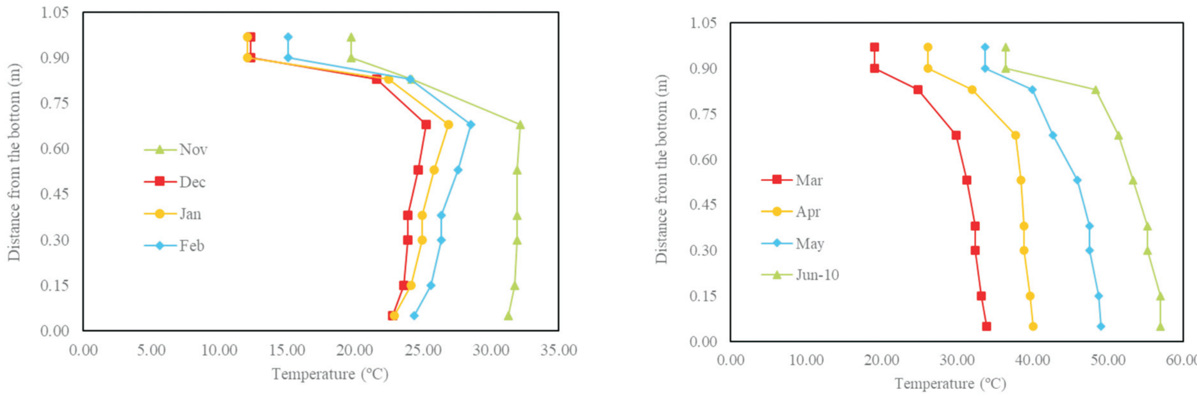

(a) (b)

Fig. 15. Distribution of temperature with the depth (a) The period November-February. (b) The period March-June.

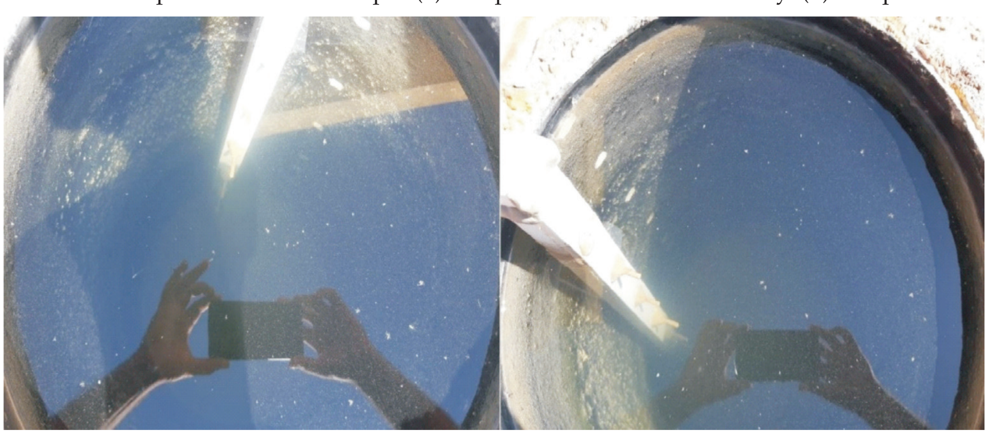

Fig. 16. Sunny area within the pond (a) after March (b) before March.

The highest temperature recorded was 59 ºC in June. The small surface area had a significant impact on the performance of solar ponds, especially for the period from December to March. So, the diameter of the pond should be at least twice its height to ensure that sunlight reaches the bottom.

References

Akbarzadeh, A., Andrews, J. and Golding, P. 2008. Solar ponds, in solar energy conversion and photoenergy systems. *Encycl. Life Support Syst*. Eolss Publ. Oxford, UK.

Aizaz, A. and Yousaf, R. 2013. Construction and analysis of a salt gradient solar pond for hot water supply. *Eur. Sci. J.* 9 : (36).

Andrews, J. and Akbarzadeh, A. 2005. Enhancing the thermal efficiency of solar ponds by extracting heat from the gradient layer. *Sol. Energy.* 78 (6) : 704–716.

Date, A. and Akbarzadeh, A. 2013. Salinity gradient solar ponds. In: Napoleon, E., Akbarzadeh, A. (Eds.), *Energy Sciences and Engineering Applications*. CRC press. E.Book.

Hassairi, M., Safi, M. J. and Chibani, S. 2001. Natural brine solar pond: an experimental study. *Sol. Energy.* 70 (1): 45–50.

Hull, J. R. 1986. Solar ponds using ammonium salts. *Sol. Energy.* 36 (6) : 551–558.

Hull, J.R., Nielsen, C.E. and Golding, P. 1988. *Salinity Gradient Solar Ponds.* CRC Press, Florida.

Kurt, H., Ozkaymak, M. and Binark, A. K. 2006. Experimental and numerical analysis of sodium-carbonate salt gradient solar-pond performance under simulated solar-radiation. *Appl. Energy*. 83 (4) : 324–342.

Leblanc, J., Akbarzadeh, A., Andrews, J., Lu, H. and Golding, P. 2011. Heat extraction methods from salinity-gradient solar ponds and introduction of a novel system of heat extraction for improved efficiency. *Sol. Energy.* 85 (12) : 3103–3142.

Murthy, G. R. and Pandey, K. P. 2002. Scope of fertiliser solar ponds in Indian agriculture. *Energy.* 27(2) : 117–126.

Ochs, T. L., Johnson, S. C. and Sadan, A. 1981. Application of a salt gradient solar pond to a chemical process industry," *Proc. Annu. Meet.-Am. Sect. Int. Sol. Energy Soc.*;(United States), 4, no. CONF-810509-(Vol. 1).

Sayer, A.H., Al-Hussaini, H. and Campbell, A. N. 2017. Experimental analysis of the temperature and concentration profiles in a salinity gradient solar pond with, and without a liquid cover to suppress evaporation. *Sol. Energy*. 155 : 1354–1365.

Suarez, B., Gonzalez-Pedro, V., Ripolles, T. S., Sanchez, R. S., Otero, L. and Mora-Sero, I. 2014. Recombination study of combined halides (Cl, Br, I) perovskite solar cells. *J. Phys. Chem. Lett.* 5 (10) : 1628–1635.

Tabor, H. 1979. SOLAR PONDS (NON-CONVECTIVE). *Solar Energy Conversion*. 167–183.